AIAA JOURNAL
Vol. 44, No. 5, May 2006

Flow Around a Rotatable Square Cylinder–Plate Body

Mustafa Sarioğlu*
Karadeniz Technical University, 61080 Trabzon, Turkey
Yahya Erkan Akansu†
Niğde University, 51200 Niğde, Turkey
and
Tahir Yavuz‡
Karadeniz Technical University, 61080 Trabzon, Turkey

The flow around a square cylinder with a plate attached to it has been investigated experimentally in the Reynolds number range between 7.5×10^3 and 5.5×10^4. The plate was located at the center of the front face of the square cylinder at the beginning. To determine the effects of the incidence angle of the square cylinder–plate body on the pressure distributions and vortex shedding, the square cylinder with the plate was rotated. The incidence angle was varied from 0 to 180 deg, corresponding to the position of the plate in the front and back face of the cylinder, respectively. The width of the cylinder and the plate were chosen to be the same at 28 mm. Measurements of shedding frequency and pressures on the surface of the cylinder were obtained. The results indicate that the Strouhal number based on D, the side length of the square cylinder, has a strong peak at $\theta = 12$ deg. After that, it decreases and remains nearly constant in the range from 50 to 105 deg. Two weaker peaks have also been observed at $\theta = 112$ and 162 deg. The positions of flow attachments, separations, and reattachments on the square cylinder due to the attached plate and the inclination of the body have been clearly obtained from the pressure distributions on the square cylinder and from the flow visualization photographs. Also, drag and lift coefficients of the square cylinder are calculated from the pressure distributions. Drag coefficient of the square cylinder has minimum and maximum values at approximately $\theta = 20$ and 80 deg, respectively, whereas the lift coefficient has a minimum and a maximum at approximately $\theta = 110$ and 150 deg, depending on the plate position. The reducing effects of the plate on the drag and lift forces are discussed.

Nomenclature

C_D	=	drag coefficient of square cylinder based on D as reference length
C_L	=	lift coefficient of square cylinder based on D as reference length
C_p	=	pressure coefficient
D	=	side length of square cylinder
D'	=	projected cross-stream dimension of square cylinder/plate body
f	=	vortex-shedding frequency
L	=	width of plate
P	=	surface pressure
P_∞	=	static pressure of freestream
Re	=	Reynolds number based on D, $U_0 D/\nu$
Sr	=	Strouhal number, fD/U_0
Sr'	=	Strouhal number, fD'/U_0
U_0	=	freestream velocity
x, y	=	streamwise and lateral coordinates, measured from center of cylinder
θ	=	inclination angle of square cylinder/plate body
ν	=	kinematic viscosity of air
ρ	=	density of air

Received 7 June 2005; accepted for publication 3 November 2005.

*Assistant Professor, Department of Mechanical Engineering; sarioglu@ktu.edu.tr.
†Research Assistant, Department of Mechanical Engineering; akansu@nigde.edu.tr.
‡Professor, Department of Mechanical Engineering; tyavuz@ktu.edu.tr.

I. Introduction

MANY researchers have been interested in the study of flow past bluff bodies for a long time because of the intrinsic complexities and importance of these flows in many practical engineering applications, such as the designs of chimneys, suspension bridges, tower structures, road vehicles, tall buildings, heat exchangers, etc. Numerous works on flow past a bluff body have been reported in the literature.

The occurrence of vortex shedding from a single square cylinder depends on freestream flow characteristics and the angle of incidence to the flow. For a square cylinder at the angle of incidence in the range of $0 \leq \theta \leq 45$ deg, large amounts of data concerning pressure distribution, vortex shedding, and drag coefficient have been provided by a number of authors.[1–7] These results essentially classified the flow around a square cylinder into two patterns. The first flow pattern is up and beyond the angle at about 13 deg where a sudden jump occurred in the Strouhal number. For $\theta < 13$ deg, a shear layer separated at the leading edge does not reattach on the lower side face of the cylinder.[1] The other flow pattern, where reattachment of the separated shear layer was indicated, took place beyond this angle. Chen and Liu[2] related the combined influence of the Reynolds number and angle of incidence on the patterns of separated shear layer and vortex formation. For low Reynolds numbers, $Re = 2.0 \times 10^3$–3.3×10^3, the occurrence of a jump in Strouhal number was at relatively higher angle of 17 deg.

In many applications, bluff bodies are often subject to the influence of another object. It is well known that two bodies that are closely placed in a tandem arrangement in a flow show strong aerodynamic interference with each other because of the effects of the wake generated by the upstream body. For this reason, pressure distributions and vortex shedding patterns of bodies in arrangement are thoroughly different from those of the individual bodies. A small rod upstream of a bluff body can be used for drag reduction to control the flow around the bluff bodies. Also, the frontbody shape or afterbody shape of bluff bodies can change considerably the behavior of the flow around the bodies. On the other hand, the wake flow

of a bluff body can be considerably changed by a splitter plate.[8] A splitter plate either attached or placed at a certain distance in the wake of bluff bodies can reduce the drag and the strength of the vortex shedding. The effects of length of a splitter plate, attached to the body, on the flow around a bluff body have been investigated by Gerrard,[9] Apelt et al.,[10] and Apelt and West,[11] among others.

Gerrard[9] examined the frequency of vortex shedding from a circular cylinder with splitter plates of different lengths up to a maximum of $2D$ attached to the cylinder. As the splitter plate length was increased, the Strouhal number was found to decrease to a minimum for a plate length of approximately $1D$ and then to increase as the splitter plate length was increased to $2D$. The study by Apelt et al.[10] concluded that splitter plates reduce the drag markedly by stabilizing the separation points and produce a wake narrower than that for a plain cylinder, raise the base pressure by as much as 50%, and affect the Strouhal number to a lesser degree. In the study by Nakamura,[12] vortex shedding from various shaped bluff bodies, such as a circular cylinder, semicircular section model with and without a $\frac{2}{1}$ rectangular block, ⊦, and H section models with splitter plates were experimentally investigated. It was shown that vortex shedding from bluff bodies with extended splitter plates is characterized by the impinging shear-layer instability, where the Strouhal number in terms of splitter plate length increases stepwise with increasing splitter plate length.

In the study by Anderson and Szewczyk,[13] flow visualization, hot-wire, and base pressure measurements were conducted for an investigation of the near wake of a circular cylinder at subcritical Reynolds numbers between 2.7×10^3 and 4.6×10^4. A base-mounted splitter plate allowed for the modification of the formation region characteristics without disrupting the normal von Kármán shedding. The results provide an explanation for the nonlinearity in the relationship between shedding frequency and splitter plate length. An experimental investigation was carried out to study the effect of a splitter plate on the two-dimensional wake of a rectangular cylinder with fixed separation points.[14] This experimental study has shown that the characteristics of the wake downstream of the cylinder with fixed separation points can be considerably altered by placing a splitter plate on the wake centerline downstream of the cylinder. The effect of splitter plates on the wake flow characteristics of the rectangular cylinder with a splitter plate shows a relatively small effect of the Reynolds number.

Some of the experimental works introduced the flow, drag, and vortex characteristics about a freely rotatable cylinder/plate body, so that the system is an equilibrium stage where the splitter plate has freely positioned itself at the equilibrium angle.

The flow in the wake of a freely rotatable circular cylinder with a splitter plate has been investigated experimentally by Cimbala and Garg.[15] Smoke-wire flow visualizations were compared for three cases: 1) a plane cylinder, 2) a cylinder with a splitter plate $1D$ long and fixed parallel to the freestream direction, and 3) the same cylinder/splitter plate body but freely rotating. In case 3, the flow rotated to a stable angle of approximately 22 deg for a Reynolds number of 7.5×10^3, and it also revealed that the wake of the freely rotatable cylinder/splitter plate body is not grossly different from that of the plain cylinder. When fixed at 0 deg, however, the splitter plate significantly alters the wake. Specifically, the fixed splitter plate forces a delay in the formation of the von Kármán vortex street. The behavior of a circular cylinder with an attached splitter plate under conditions where the entire cylinder/splitter plate body was free to rotate about the cylinder axis has been studied experimentally by Cimbala and Chen.[16] It has been observed that a cylinder/splitter plate model rotates to an equilibrium position off of the centerline at both subcritical and supercritical Reynolds numbers. For any given L/D, the equilibrium angle decreases suddenly in the transitional Reynolds number regime, where the boundary-layer separation on the cylinder changes from laminar to turbulent. At supercritical Reynolds numbers, angle θ (starting from the back base point of the cylinder) rises slowly and then levels off at very high Reynolds numbers to a value significantly smaller than that at subcritical Reynolds numbers. It was found that the transition Reynolds number range for the cylinder with very short plate lengths, $L/D \approx \frac{1}{8}$, was around 2.5×10^5 to 3.5×10^5. For longer splitter plate lengths, the critical Reynolds number was lower; the transition Reynolds number range was around 1.5×10^5 to 2×10^5. Also, in the study by Cimbala and Leon,[17] the drag of freely rotatable cylinder/splitter plate body at subcritical Reynolds numbers was introduced for various splitter plate lengths.

Rathakrishnan[18] measured the drag coefficient of a rectangular bluff body (the ratio of $h/L = 1.2$, where h and L are the height and length of the rectangular cylinder) with a splitter plate placed in front of and behind the body at the midplane and off-center locations. He also considered the effect of the length of the splitter plate and the pitch sensitivity of the bluff-body/splitter plate combination in the range from -15 to $+15$ deg. It was concluded that, for a bluff bodies with splitter plates, a mechanism other than near-wake manipulation might exist for drag reduction and for altering the vortex-shedding characteristics. For centerline positioning, a backward splitter plate is more effective in drag reduction, whereas for $h/4$ positioning from the top, the forward plate gives less drag. The splitter plate is most effective when the pitch angle is zero.

Texier et al.[19] studied the influence of a short separating element placed on the median axis of a uniform flow downstream and upstream a half-circular cylinder for various gaps. The flow recirculation rate, the swirling roughness, and propagation were examined by velocity field measurements and flow visualization analyses.

The study by Fleck[20] aimed to measure the excitation frequencies in the lift force on a model of a combined circular–rectangular prism placed in a crossflow at angle of attack.

In the study by Wei and Chang,[21] flow characteristics of wake and base bleed flow downstream of two bluff bodies with different cross-sectional geometries, arranged side by side, were investigated. In the case of the square cylinder and flat plate in contact with each other, the frequency and spectrum of vortex shedding signals in the wake of the flat plate side and of the square cylinder side are the same. The shedding frequency of this two-body arrangement is about one-half of the average of the frequencies of the single flat plate and of the single square cylinder.

Akansu et al.[22] investigated experimentally the behavior of a stationary circular cylinder with an attached plate, under conditions where the entire cylinder/plate body was to rotate about the cylinder axis at a Reynolds number of 2×10^4. The results indicate that the shedding frequency was nearly constant in the range of 50–120 deg, and as the angle is further increased from 120 to 160 deg, it strikingly increases and then decreases again at angles greater than 160 deg. The plate also causes important changes in pressures on the surface of the cylinder as the inclination angle is increased.

In the present study, following the experimental work by Akansu et al.,[22] in which a stationary circular cylinder with attached a plate was used, flow characteristics around the square-cylinder/plate body with various inclination angles are investigated. Detailed measurements of the surface pressures and vortex shedding frequency were conducted and drag and lift coefficients were calculated. To gain a clear understanding of the attached plate effects, flow visualizations were also carried out.

II. Experimental Apparatus and Procedure

The experiments were conducted in the test section of a low-speed, open-type wind tunnel. The test section measures 289 mm wide, 457 mm high, and 1830 mm long. The two side Plexiglas® walls of the test section are tapered with a divergence angle of 0.3 deg on each side to give constant static pressure and to compensate for boundary-layer growth along the tunnel axis. Details involving the test section can be found in the paper by Sarioglu and Yavuz.[7] At the maximum tunnel speed of about 36 m/s, the freestream turbulence intensity was about 0.5%. The Reynolds number was in the range from 7.5×10^3 to 5.5×10^4 in the study, corresponding to a freestream velocity of about 4–30 m/s, respectively. The tunnel and test section are shown in Fig. 1. The square cylinder was centered at the midheight of the test section and spanned the width of the test section. The configuration of the square cylinder with an attached plate is shown in Fig. 2. The side length of the square cylinder tested, D, was 28 mm, and the width of the plate, which was made

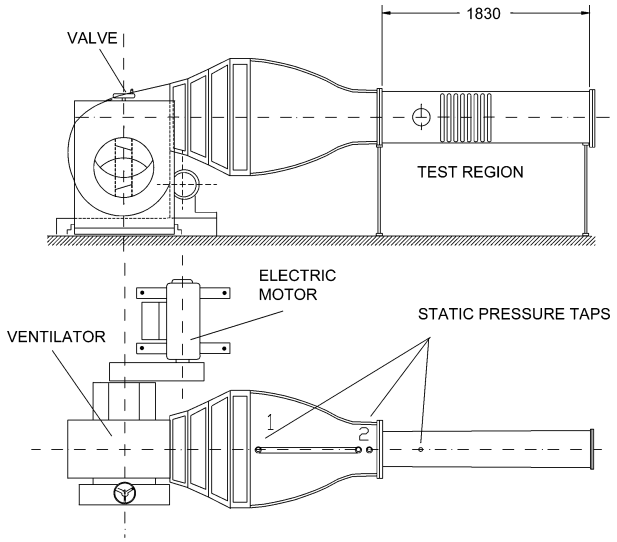

Fig. 1 Low-speed, open-type wind tunnel and test section.

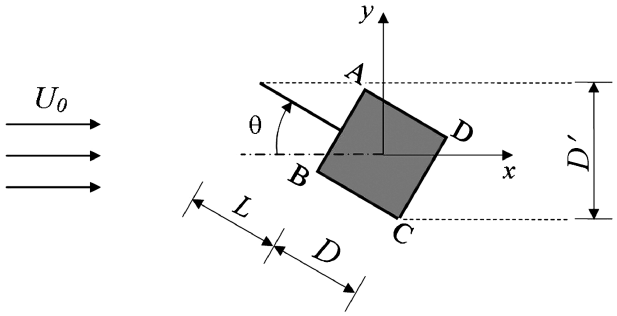

Fig. 2 Flow configuration and symbol definition.

of stainless steel, and which was attached to the cylinder was also 28 mm, that is, $L/D = 1.0$, and its thickness was 1 mm. The square cylinder has eight pressure taps 0.7 mm in diameter distributed at equal spacing on each surface AB, BC, CD, and DA, corresponding to the front, bottom, back, and upper surfaces. The angle θ defined in Fig. 2 is the inclination angle of the square cylinder/plate body. The cylinder/plate body was positioned at an angle of incidence to the freestream flow direction and turned in the range of $0 \leq \theta \leq 180$ deg with an accuracy of ± 0.5 deg.

Vortex shedding from the cylinder/plate body was detected by using a TSI intelligent flow analyzer (IFA 100) model constant temperature anemometer with two hot-film probes. The hot-film probes were calibrated using a TSI Model 1125 calibrator. The frequency response for the hot-film probes were found to be about 20 kHz by using a square wave test. The Strouhal numbers for the vortex shedding from the model were determined from the frequency analysis of the velocity fluctuations. One of the probes was located at the position of $x = 7D$, $y = 1.5D$ downstream of the body, and the other probe was used as a movable probe. Pressure measurements were made with a pressure transmitter in conjunction with a TSI Model 157 signal conditioner. The transmitter was connected to the pressure taps in reference to the freestream wall pressure.

Velocity and pressure measurements were carried out by using a computer-controlled data acquisition system. For velocity measurements at each measurement point, 2048 data points were acquired at a sampling rate of 1 kHz using a low-pass filter setting of 300 Hz. Thus, the measuring time corresponded to 2.0486 s. The pressure signals were acquired at a rate of 200 sample/s and low-pass filtered at 100 Hz. Each of the mean pressures was obtained by means of integrating the time history of 2048 data points for over 10 s. TSI Thermal-Pro Software was used to acquire signals with a 12-bit A/D converter and to obtain the statistical results of these signals. The experimental uncertainty in the measurement of velocity was determined to be less than $\pm 3\%$, whereas that of pressure was determined to be less than $\pm 4\%$. The uncertainties in the drag coefficient,

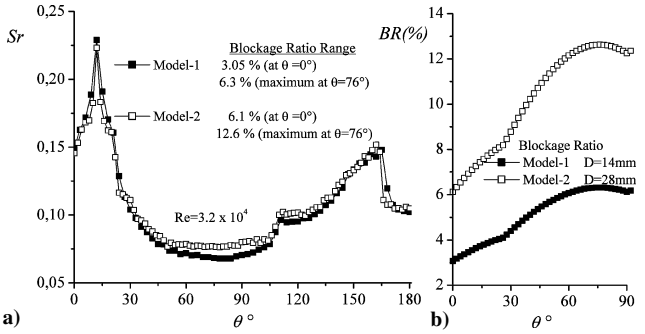

Fig. 3 Effect of blockage ratio on Strouhal number distribution.

the Strouhal number, and the frequency spectra calculated from the experimental measurements were determined to be less than ± 4.7, ± 3.3, and $\pm 1\%$, respectively.

The blockage ratio of the square cylinder/plate body with respect to the test section was 6.1% at $\theta = 0$ deg. As the body was rotated, the blockage ratio increased up to its maximum value of 12.6% at $\theta = 76$ deg. As discussed by West and Apelt,[23] the effect of blockage on time-averaged drag was unaffected by a blockage ratio less than 6%, and there is a small effect of blockage at ratios between 6 and 12%. In their results for circular cylinder, the drag coefficient changed from 1.225 to 1.275 in the range of the blockage ratio. Also, Igarashi's work[1] shows that the Strouhal number for a square prism at $\theta = 0$ deg, as a sharp-edged body, changed from 0.13 to 0.14 for the blockage ratio between 5 and 10%. Consequently, in the present study it was concluded that the blockage effect in the results is expected to be small and that the changing geometry with angle of incidence has a major influence on the results.

To substantiate the small effect of the blockage ratio, the experiments were carried out for two models having the diameters of 14 (model 1), and 28 mm (model 2), at the same Reynolds number. Results are shown in Fig. 3. Figure 3b shows the blockage ratio changes of these two models with angle of incidence, and Fig. 3a shows Strouhal number distributions. As seen in Fig. 3a, there are no considerable differences between the results obtained for the model 1 and model 2 in the Strouhal number distributions. The Strouhal number varies from 0.068 to 0.077 in the case of maximum blockage ratios of the models (6.3% for model 1 and 12.6% for model 2 at $\theta = 76$ deg). Therefore, it was concluded that the blockage effects on the Strouhal number distribution in this study are negligible.

III. Experimental Results and Discussion

A. Flow Visualization

To examine the flowfield about the cylinder/plate arrangement, flow visualization experiments were conducted by using a smoke-wire method in the wind tunnel for $Re = 7.5 \times 10^3$ (Fig. 4). In Fig. 4, the positions of flow attachment, separation, and reattachment on the square cylinder/plate body due to the attached plate and the inclination of the body can be clearly seen. The variation of vortex formation region behind the body can be also seen in Fig. 4. For $\theta = 0$ deg, the wake of the cylinder/plate body is not completely different from that of the cylinder alone. In these two cases, the flow separations occur on the upper and lower front corners. However, the wake of the cylinder/plate body at $\theta = 0$ deg is narrower than that of the cylinder alone. Increasing the angle of incidence at about $\theta = 10$ deg, the shear layer separated from the edge of the plate reattaches on the upper side of the front face. Whereas the shear layer passing the underside of the body separates from corner C up to $\theta = 105$ deg, after this angle it begins to separate from corner D. As the angle of incidence is further increased, the shear layers passing above the body do not attach on the plate.

When the cylinder alone is compared with the cylinder/plate body at $\theta = 180$ deg, there are considerable changes in the wake, and the distance required for vortex formation behind the body varies. As shown in Fig. 4, while the projected cross-stream height is increasing, the width of the wake increases.

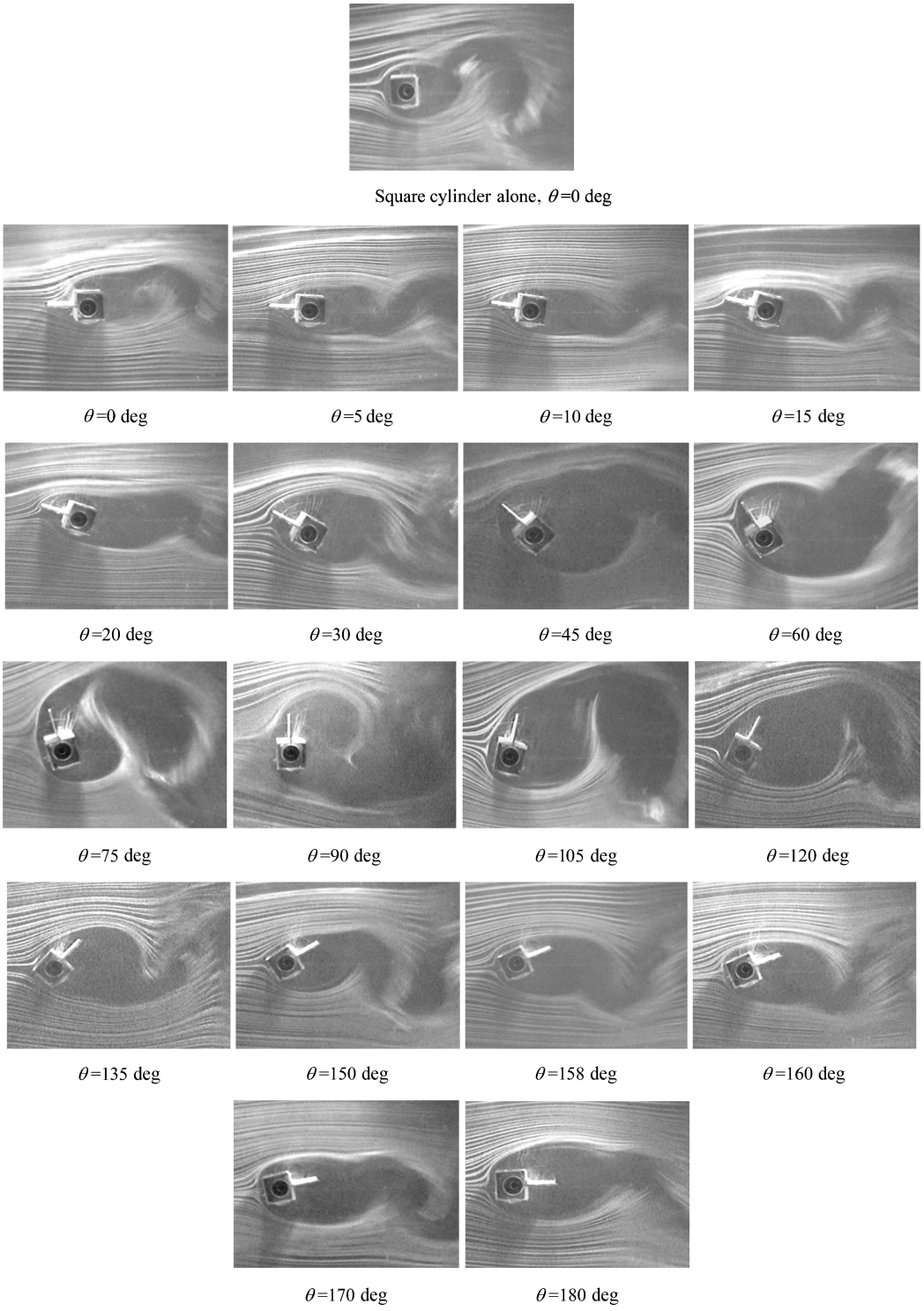

Fig. 4 Smoke-wire photographs of flow around square cylinder–plate body for $Re = 7.5 \times 10^3$.

B. Mean Pressure Distributions

Measurements of surface pressure were carried out on the surfaces of the square cylinder. The pressure coefficient C_p was defined as $C_p = (P - P_\infty)/\frac{1}{2}\rho U_0^2$. The mean pressure distributions on the surface of the cylinder with and without a plate were obtained at a Reynolds number of 3.2×10^4 for the angles of the square cylinder/plate body θ in the range 0–180 deg as shown in Fig. 5. Sign conversions of the pressures in Fig. 5 are zero on the square frame (boundary), positive inside the square, and negative outside of the square.

Pressure distribution on the front surface (AB) of the square cylinder without the plate is parabolic and has positive values. At the stagnation point on the center of the front face (AB), the C_p value equals 1. Because of the separating shear layers from the upper and lower front edges, pressures on the other faces (BC, CD, and DA) have negative values. For $\theta = 0$ deg, with the plate, the shape of the pressure profile on the AB face changes, and pressure values decrease. On the face CD, there is pressure recovery because of shifting of the location of vortex formation of the square cylinder downstream, indicating a narrower wake compared with that of without the plate. (See flow photographs in Fig. 4.) At $\theta = 10$ deg, the shear layer separated from the edge of the plate reattaches on the upper half of face AB near corner A, whereas the stagnation point occurs on the lower half of face AB and the shear layer separated

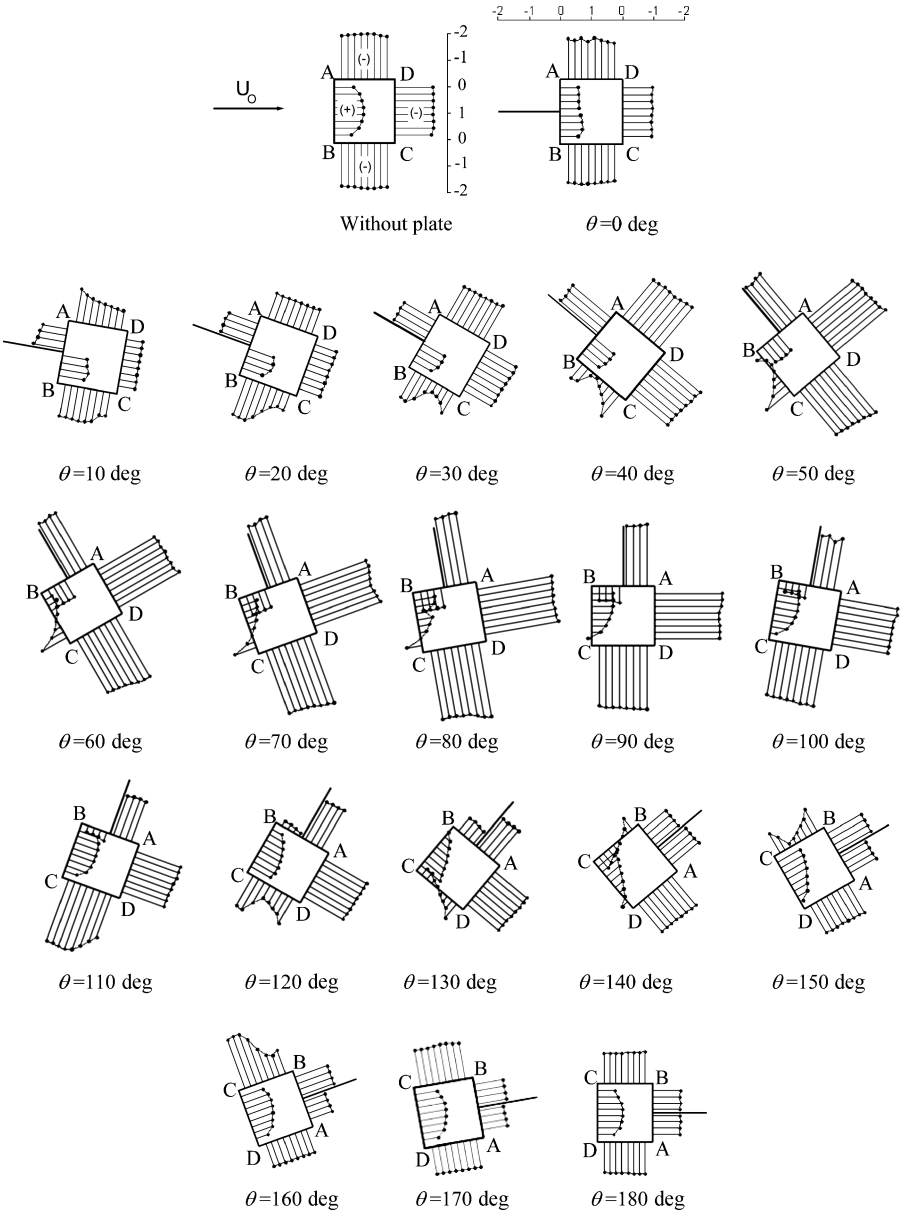

Fig. 5 Surface pressure distributions around square cylinder–plate body, $Re = 3.2 \times 10^4$.

from corner B begins to reattach near corner C. When the pressure distribution and the related photograph for $\theta = 10$ deg are examined, the wake is narrowest, and this causes maximum pressure recovery on face CD. The pressure distribution on face BC varies with the rotation of the cylinder/plate body. As θ increases up to $\theta = 50$ deg, the position of the reattached shear layer shifts from corner C to corner B. Direct attachment of the oncoming flow begins to occur on face BC at $\theta = 60$ deg. Because the projected dimension is increased, the width of the wake increases. Therefore, pressure values on the surfaces remaining inside the wake region drop to values below that measured in the case without a plate at zero angle of incidence.

Whereas the values of the pressures on the half part near corner B on face AB are positive up to $\theta = 110$ deg, they become negative due to the separation of the shear layers from corner B to the upside direction.

This indicates that this shear layer reattached to the plate and a bubble probably occurs between corner B and the plate. In the range $100 \leq \theta \leq 130$ deg, because of direct attachment of the oncoming flow, the pressures on the entire face BC are positive.

When the pressure distribution on face CD is examined, it can be said that face CD is under the effect of the wake region up to $\theta = 100$ deg. After $\theta = 100$ deg, the shear layer separated from corner C begins to reattach on face CD near corner D. As θ is increased further, the point of reattachment shifts to corner C. When $\theta = 130$ deg, freestream attachment begins on face CD. From $\theta = 150$ deg on, the attachment of the freestream occurs only on the entire face CD, and the stagnation point is seen near corner C on this surface. In this case, the flow separations occur from corners C and D. However, only the shear layer separated from corner C reattaches on face BC at $\theta = 150$ and 160 deg. In the case of $\theta = 180$ deg, for which the plate is in the wake of the cylinder, the pressure on the base of the cylinder has higher value compared with the values obtained for the case without a plate. In this case, vortices behind the cylinder are formed farther downstream in the wake of the cylinder.

C. Spectral Measurements and Strouhal Numbers

Spectra measured at different angles of incidences between 0 and 180 deg are presented in Fig. 6. They were obtained at the position $x/D = 4$, $y/D = 2.5$ in the wake of the square cylinder to preclude interference in the velocity signal from vortices of opposite signs. As shown in Fig. 6, with an increase of θ from 0 deg, there is a gradual increase in vortex-shedding frequency up to $\theta = 12$ deg, whereas

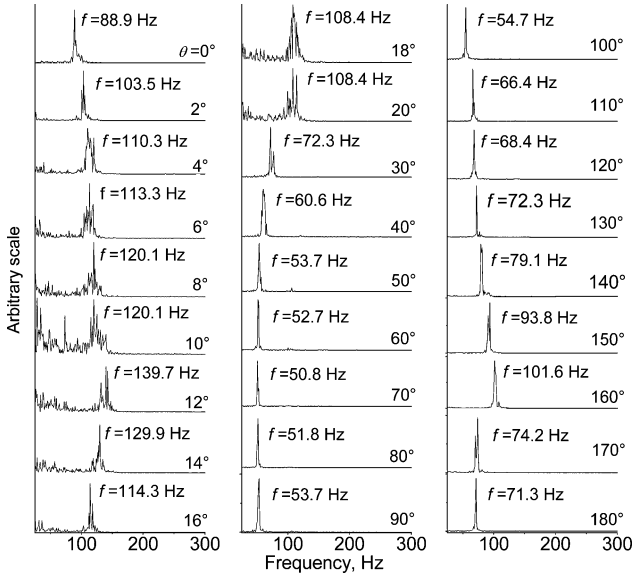

Fig. 6 Spectra measured at $x/D = 4$, $y/D = 2.5$ in wake of square cylinder–plate body, $Re = 3.2 \times 10^4$.

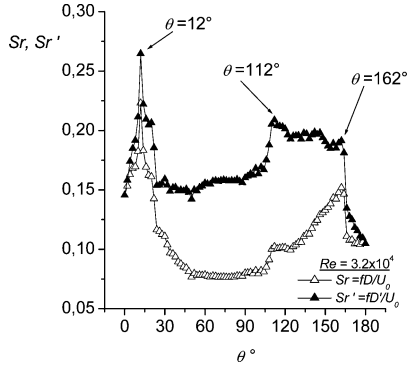

Fig. 7 Strouhal number vs incidence angle θ.

there is a considerable decrease at 14–40 deg. The vortex-shedding frequency remains almost constant in the range $50 \leq \theta \leq 100$ deg. With a further increase in θ, the frequency increases strikingly at 110–160 deg and then decreases again.

Strouhal numbers Sr and Sr', calculated using vortex-shedding frequencies obtained from spectral distributions, are shown in Fig. 7. Sr' values calculated by using the projected cross-stream dimension of the square cylinder/plate body D' eliminate the effects due to the variation of the projected height and include only the effects that proceed from the angle of incidence, whereas Strouhal number values calculated using D include both of these effects. As shown in Fig. 7, the Strouhal number has a strong peak at $\theta = 12$ deg, after which it decreases and remains nearly constant in the range of $\theta = 50$–105 deg. Two weaker peaks have also been observed at $\theta = 112$ and 162 deg. When the Strouhal numbers are examined together with the pressure distributions at $\theta = 10$ and 15 deg, the increase in the Strouhal number at $\theta = 12$ deg is associated with the reattachment on face BC of the shear layer separated from corner B. A similar explanation can be given for the increases in the Strouhal number at $\theta = 112$ and 162 deg. At $50 \leq \theta \leq 105$ deg, the Strouhal number keeps constant because the structure of the flow around the body is not changed and the projected height of the body is not considerably varied. As a matter of fact, in this range of θ, the values of Strouhal numbers and Sr' do not change considerably with θ, as seen in Fig. 7.

Figure 8 shows a comparison between the present study and the results derived by Knisely[5] for a rectangular cylinder. Just as there is a sudden jump at $\theta = 12$ deg, there is also a sharp increase in Sr' at $\theta = 112$ deg. This is associated with the reattachment on surface

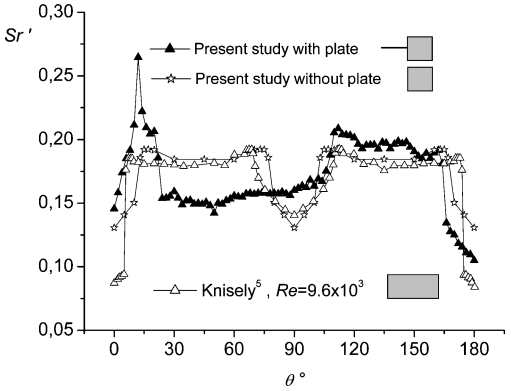

Fig. 8 Comparison of Sr' with that in the literature.

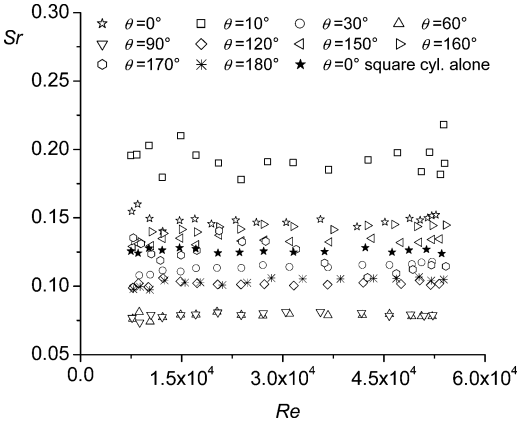

Fig. 9 Distribution of Strouhal number of cylinder–plate body vs Reynolds number for different angles of incidence.

CD close to corner D. In the case of the plate being downstream of the body, a characteristic of Sr' is that it is similar to those of both the square cylinder alone and the rectangular cylinder between 90 and 180 deg, as shown in Fig. 8. The reason for the sharp drop in Sr' after $\theta = 162$ deg is that the shear layer separated from corner C, corresponding to the upper leading edge of the body, does not reattach on surface BC any longer.

Figure 9 shows the Strouhal number as a function of the Reynolds number for various considered angles of incidence. Data were acquired at about 18 different wind-tunnel speeds, giving a Reynolds number range from about 7.5×10^3 to 5.5×10^4 for each angle of incidence θ. For a given angle of incidence, especially at $\theta > 10$ deg, the Strouhal number was found to be largely independent of the Reynolds number. In the case of $\theta = 10$ deg, the Strouhal number has an unstable variation with the Reynolds number. At this angle of incidence the reattachment of the shear layer separated from corner B just begins to occur on the square cylinder as seen in Fig. 5.

Figure 10 shows a comparison between the results of some previous studies and the present result for the square cylinder alone at $\theta = 0$ deg and for the square cylinder with the plate at $\theta = 0$, 90, and 180 deg. As shown in Fig. 10, the present results for the square cylinder alone at $\theta = 0$ deg agree well with the results determined by Igarashi[1] and Obasaju.[4]

D. Drag and Lift Coefficients

The drag and lift coefficients of the square cylinder are obtained, at a Reynolds number of 3.2×10^4, by the integration of the mean pressure distributions on the cylinder as shown in Figs. 11 and 12. Hence, results include the effect of the plate. The contributions to drag and lift coefficients due to the effects of the plate are not considered. As shown in Fig. 11, for the square cylinder/plate body, depending on the pressure distributions obtained with 10-deg increment, the drag coefficient decreases with an increasing angle of incidence and reaches a minimum value at $\theta = 20$ deg. At

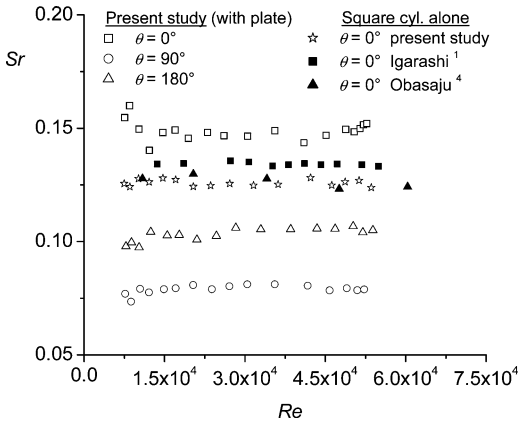

Fig. 10 Variation of Strouhal number vs Reynolds number for comparison with previous studies.

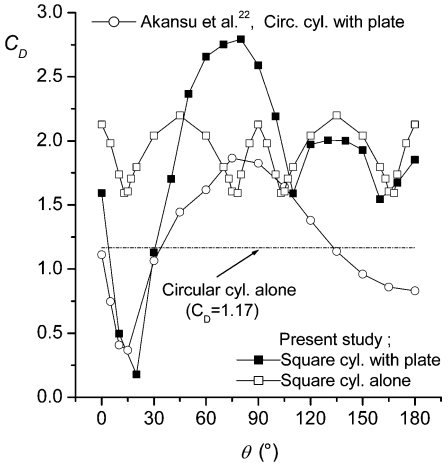

Fig. 11 Drag coefficient of square cylinder vs θ.

$\theta = 0$ deg, the drag coefficient decreases by approximately 25% compared with that of the square cylinder alone. The drag coefficient drops considerably with the rotation of the body to 10 and 20 deg because the pressure on the upper half part of face AB becomes negative and because the base pressures are recovered. The minimum value of the drag coefficient is approximately 10% of that of the square cylinder alone at $\theta = 20$ deg. After 20 deg, with a further increase of the angle of incidence, the width of the wake increases, causing a striking decrease in C_p to a value of -2.5. Consequently, the drag coefficient increases sharply up to 80 deg.

Because of the influence of the plate on the pressure difference between the front and back surfaces of the body, C_D values are higher than that of the square cylinder alone in the range of 50–100 deg. After $\theta = 80$ deg, with recovery the pressures on the back region of the body and a decrease of the width of the wake region, C_D begins to decrease again until 110 deg. When $\theta = 120$ deg, because of the recovery of the pressure on face CD and the change in direction of the pressure on the half part closer to corner B on face AB from positive to negative, drag coefficients increase to a value of about 2.0 and remain constant up to 150 deg. At $\theta = 160$ deg, the drag coefficient decreases again due to decreasing pressure on face BC and recovery of the pressure on face DA. Then, at 180 deg, the drag coefficient reaches a value of 1.85 below 2.13, the value of the square cylinder alone at $\theta = 180$ deg. Figure 11 also shows the results found by Akansu et al.[22] for the circular cylinder with plate. As seen in Fig. 11, with the angle of incidence up to 90 deg, the plots show similar trends when the results for the circular cylinder are compared. However, it can be seen clearly that after $\theta = 90$ deg, the influence of the plate on the square cylinder reduces, and the variation of drag coefficients of the square cylinder with plate has a similar trend with that of the square cylinder alone.

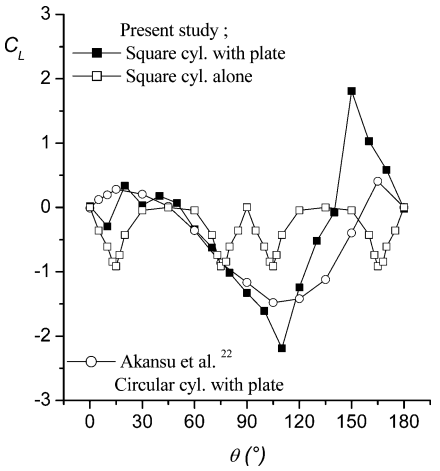

Fig. 12 Lift coefficient on square cylinder vs θ.

Figure 12 shows lift coefficients of the square cylinder with and without a plate as well as those determined by Akansu et al.[22] for a circular cylinder with a plate. With an increase in θ from 0 deg for the square cylinder, the balance in the vertical components of the pressure forces on all faces of the square cylinder break, and, thus, a lift force acting on the cylinder occurs. As shown in Fig. 12, C_L values are about zero between 0 and 50 deg. With increasing θ, C_L decreases and reaches its minimum value of -2.19 at 110 deg. In the range of $\theta = 60$–90 deg, the positive pressures acting on face BC affect the upward direction, but after $\theta = 90$ deg, they reverse effects. Therefore, the lift coefficient continues to reduce up to 110 deg. When the pressure distribution at the angle of incidence $\theta = 120$ deg is examined, there is a pressure recovery formed by means of the flow reattachment on face CD, and the pressures on the half-part closer to corner B on face AB convert from positive to negative. Thus, the lift coefficient begins to increase. Although there is a geometric asymmetry because of the balance among the pressures on all of the surfaces of the cylinder, there is no lift at $\theta = 140$ deg. The lift coefficient has a maximum value at $\theta = 150$ deg. After this point, C_L decreases again and reaches a zero value at $\theta = 180$ deg by means of symmetry about the centerline of the body. When the drag coefficients of the square cylinder–plate body are compared with those of the circular cylinder/plate body, especially in the cases of the plate having a bigger projected cross-stream dimension, the square cylinder/plate body behaves as a bluff body and the lift coefficients of the square cylinder/plate body show a similar trend with those of the circular cylinder/plate body.

IV. Conclusions

The flow around a square cylinder with a plate attached to it has been investigated experimentally in the Reynolds number range from 7.5×10^3 to 5.5×10^4. At different angles of θ, the influences of the plate on the pressures measured on the surface of the square cylinder, drag and lift coefficients, and vortex-shedding phenomena are examined.

Pressure distributions on the square cylinder change considerably depending on the angle of incidence. For some ranges of angle of incidence, $\theta = 10$–50, 110–120, and 150–160 deg, the pressure distributions on the faces of the square cylinder where the reattachments occur exhibit a strong recovery. At the angles of incidence where the plate attached to the square cylinder behaves as a bluff body, the wake region enlarges, and this causes an important decrease in the base pressures. When the plate acts as a splitter plate, the wake region narrows, and this leads the base pressures to recover.

At $\theta = 12$ and 112 deg, a rapid rise in Strouhal number is obtained because the shear layer separated from the lower leading edge of the square cylinder just begins to reattach near the lower trailing edge on the lower face. Similarly, after $\theta = 162$ deg, there is a sharp decrease in Strouhal number. This is associated with the ending of the reattachment on the upper face of the cylinder. Over the Reynolds

number range 7.5×10^3–5.5×10^4, Strouhal numbers were found to be independent of the Reynolds number, and the flow structure changed only with the angle of incidence.

Because of pressure differences between the front and back and upper and lower sides of the body, drag and lift coefficients changed with incidence. At zero incidences, the drag coefficient decreases about 25% compared with that of the square cylinder alone. The drag coefficient has a minimum value of 0.18 at 20 deg and a maximum value of 2.8 at 80 deg, whereas it has a value of 2.13 in the case of the square cylinder alone. The lift coefficient has a zero value at 0 and 180 deg due to symmetry between the upper and lower sides of the square cylinder, as in the case of the square cylinder alone, and, in addition to this, its value is approximately zero at 10–50 deg and 140 deg because of the balance among the pressures on all of the surfaces of the cylinder. C_L has a minimum value of -2.2 at 110 deg and a maximum value of 1.8 at 150 deg.

References

[1]Igarashi, T., "Characteristics of the Flow Around a Square Prism," *Bulletin of the Japan Society of Mechanical Engineers*, Vol. 27, No. 231, 1984, pp. 1858–1865.

[2]Chen, J. M., and Liu, C. H., "Vortex Shedding and Surface Pressures on a Square Cylinder at Incidence to a Uniform Air Stream," *International Journal of Heat and Fluid Flow*, Vol. 20, No. 6, 1999, pp. 592–597.

[3]Lee, B. E., "The Effect of Turbulence on the Surface Pressure Field of a Square Prism," *Journal of Fluid Mechanics*, Vol. 69, Pt. 2, 1975, pp. 263–282.

[4]Obasaju, E. D., "An Investigation of the Effects of Incidence on the Flow Around a Square Section Cylinder," *Aeronautical Quarterly*, Vol. 34, Nov. 1983, pp. 243–259.

[5]Knisely, C. W., "Strouhal Numbers of Rectangular Cylinders at Incidence: A Review and New Data," *Journal of Fluids and Structures*, Vol. 4, No. 4, 1990, pp. 371–393.

[6]Vickery, B. J., "Fluctuating Lift and Drag on a Long Cylinder of a Square Cross-Section in a Smooth and in a Turbulent Stream," *Journal of Fluid Mechanics*, Vol. 25, 1966, pp. 481–494.

[7]Sarioglu, M., and Yavuz, T., "Subcritical Flow Around Bluff Bodies," *AIAA Journal*, Vol. 40, No. 7, 2002, pp. 1257–1268.

[8]Roshko, A., "Experiments on the Flow past a Circular Cylinder at Very High Reynolds Number," *Journal of Fluid Mechanics*, Vol. 10, 1961, pp. 345–354.

[9]Gerrard, J. H., "The Mechanics of the Formation Region of Vortices Behind Bluff Bodies," *Journal of Fluid Mechanics*, Vol. 25, Pt. 2, 1966, pp. 401–413.

[10]Apelt, C. J., West, G. S., and Szewczyk, A. A., "The Effects of Wake Splitter Plates on the Flow past a Circular Cylinder in the Range $10^4 < R < 5 \times 10^4$," *Journal of Fluid Mechanics*, Vol. 61, Pt. 1, 1973, pp. 187–198.

[11]Apelt, C. J., and West, G. S., "The Effects of Wake Splitter Plates on Bluff Body Flow in the Range $10^4 < \mathrm{Re} < 5 \times 10^4$. Part 2," *Journal of Fluid Mechanics*, Vol. 71, Pt. 1, 1975, pp. 145–160.

[12]Nakamura, Y., "Vortex Shedding from Bluff Bodies with Splitter Plates," *Journal of Fluids and Structures*, Vol. 10, No. 2, 1996, pp. 147–158.

[13]Anderson, E. A., and Szewczyk, A. A., "Effects of a Splitter Plate on the Near Wake of a Circular Cylinder in 2 and 3-Dimensional Flow Configurations," *Experiments in Fluids*, Vol. 23, No. 2, 1997, pp. 161–174.

[14]Mansingh, V., and Oosthuizen, P. H., "Effects of Splitter Plates on the Wake Flow Behind a Bluff Body," *AIAA Journal*, Vol. 28, No. 5, 1990, pp. 778–783.

[15]Cimbala, J. M., and Garg, S., "Flow in the Wake of a Freely Rotatable Cylinder with Splitter Plate," *AIAA Journal*, Vol. 29, No. 6, 1991, pp. 1001–1003.

[16]Cimbala, J. M., and Chen, K. T., "Supercritical Reynolds Number Experiments on a Freely Rotatable Cylinder/Splitter Plate Body," *Physics of Fluids*, Vol. 6, No. 7, 1994, pp. 2440–2445.

[17]Cimbala, J. M., and Leon, J., "Drag of Freely Rotatable Cylinder/Splitter-Plate Body at Subcritical Reynolds Number," *AIAA Journal*, Vol. 34, No. 11, 1996, pp. 2446–2448.

[18]Rathakrishnan, E., "Effect of Splitter Plate on Bluff Body Drag," *AIAA Journal*, Vol. 37, No. 9, 1999, pp. 1125–1126.

[19]Texier, A., Bustamante, A. S. C., and David, L., "Contribution of a Short Separating Plate on the Control of the Swirling Process Downstream a Half-Cylinder," *Experimental Thermal and Fluid Science*, Vol. 26, No. 5, 2002, pp. 565–572.

[20]Fleck, B. A., "Strouhal Numbers for Flow past a Combined Circular-Rectangular Prism," *Journal of Wind Engineering and Industrial Aerodynamics*, Vol. 89, No. 9, 2001, pp. 751–755.

[21]Wei, C. Y., and Chang, J. R., "Wake and Base-Bleed Flow Downstream of Bluff Bodies with Different Geometry," *Experimental Thermal and Fluid Science*, Vol. 26, No. 1, 2002, pp. 39–52.

[22]Akansu, Y. E., Sarioglu, M., and Yavuz, T., "Flow Around a Rotatable Circular Cylinder–Plate Body at Subcritical Reynolds Numbers," *AIAA Journal*, Vol. 42, No. 6 , 2004, pp. 1073–1080.

[23]West, G. S., and Apelt, C. J., "The Effects of Tunnel Blockage and Aspect Ratio on the Mean Flow past a Circular Cylinder with Reynolds Numbers Between 10^4 and 10^5," *Journal of Fluid Mechanics*, Vol. 114, 1982, pp. 361–377.

J. Gore
Associate Editor